

Article

Direct Visualization of Spatial Inhomogeneity of Spin Stripes Order in $\text{La}_{1.72}\text{Sr}_{0.28}\text{NiO}_4$

Gaetano Campi ^{1,*}, Nicola Poccia ^{2,*}, Bobby Joseph ³, Antonio Bianconi ^{1,4}, Shrawan Mishra ^{5,6}, James Lee ⁵, Sujoy Roy ⁵, Agustinus Agung Nugroho ⁷, Marcel Buchholz ⁸, Markus Braden ⁸, Christoph Trabant ⁹, Alexey Zozulya ^{10,11}, Leonard Müller ¹⁰, Jens Viehhaus ¹⁰, Christian Schüßler-Langeheine ⁹, Michael Sprung ¹⁰ and Alessandro Ricci ^{4,10,*}

¹ Institute of Crystallography, CNR, via Salaria Km 29.300, 00015 Monterotondo, Roma, Italy

² Institute for Metallic Materials, Leibniz IFW Dresden, 01069 Dresden, Germany

³ Elettra Sincrotrone Trieste. Strada Statale 14 - km 163.5, AREA Science Park, I-34149 Basovizza, Trieste, Italy

⁴ Rome International Center for Materials Science Superstripes RICMASS, Via dei Sabelli 119A, 00185 Roma, Italy

⁵ Advanced Light Source, Lawrence Berkeley National Laboratory, Berkeley, CA94720, USA

⁶ School of Materials Science and Technology, Indian Institute of Technology, Banaras Hindu University, Varanasi 221005, India

⁷ Faculty of Mathematics and Natural Sciences Institut Teknologi Bandung, Jl. Ganesha 10 Bandung, Jawa Barat 40132, Indonesia

⁸ II. Physikalisches Institut, Universität zu Köln, Zùlpicher Str. 77, 50937 Köln, Germany

⁹ Helmholtz-Zentrum Berlin für Materialien und Energie GmbH, Institute Methods and Instrumentation in Synchrotron Radiation Research, Albert-Einstein-Str. 15, 12489 Berlin, Germany

¹⁰ Deutsches Elektronen-Synchrotron DESY, Notkestraße 85, D-22607 Hamburg, Germany

¹¹ European X-ray Free-Electron Laser Facility GmbH Holzkoppel 4, 22869 Schenefeld, Germany

* Correspondence: gaetano.campi@ic.cnr.it (G.C.); n.poccia@ifw-dresden.de (N.P.); phd.alessandro.ricci@gmail.com (A.R.)

Received: 9 July 2019; Accepted: 8 August 2019; Published: 10 August 2019



Abstract: In several strongly correlated electron systems, the short range ordering of defects, charge and local lattice distortions are found to show complex inhomogeneous spatial distributions. There is growing evidence that such inhomogeneity plays a fundamental role in unique functionality of quantum complex materials. $\text{La}_{1.72}\text{Sr}_{0.28}\text{NiO}_4$ is a prototypical strongly correlated perovskite showing spin stripes order. In this work we present the spatial distribution of the spin order inhomogeneity by applying micro X-ray diffraction to $\text{La}_{1.72}\text{Sr}_{0.28}\text{NiO}_4$, mapping the spin-density-wave order below the 120 K onset temperature. We find that the spin-density-wave order shows the formation of nanoscale puddles with large spatial fluctuations. The nano-puddle density changes on the microscopic scale forming a multiscale phase separation extending from nanoscale to micron scale with scale-free distribution. Indeed spin-density-wave striped puddles are disconnected by spatial regions with negligible spin-density-wave order. The present work highlights the complex spatial nanoscale phase separation of spin stripes in nickelate perovskites and opens new perspectives of local spin order control by strain.

Keywords: nanoscale phase separation; spin stripes; nickelates; quantum complex materials

1. Introduction

The complex organization of different orders seems to have a fundamental role in the mechanism governing the emergence of unique functionalities in quantum materials [1]. In cuprate perovskites,

the stripes phases have been the object of interest for decades [1–3], while in this last decade new scanning X-ray diffraction methods have been developed due to the ability to focus X-ray synchrotron radiation to micron and sub-micron spots. These methods have made it possible to obtain visualization of spatial topological inhomogeneity of charge density wave order in doped cuprate perovskites [4,5]. Short range generalized Wigner charge density waves have been found to be spatially inhomogeneous with the formation of “striped charge puddles” anti-correlated with competing puddles of “striped dopants rich clusters” [4–6]. These experimental results have opened a new era in the long-standing research of complexity in doped strongly correlated perovskites, since they have falsified popular stripes theories which for decades have assumed a homogeneous spatial distribution of spin stripes and charge-stripes. In this work we focus on the spin stripes phase in doped nickelate perovskites. In order to determine the role that the spatial distribution of ordered phases in cuprates plays for the superconductivity, it is instructive to study a non-superconducting reference system like the layered nickelates [7]. Keeping this idea in mind, we push forward the investigation of the spatial distribution of spin-density-wave stripes ordering (SDW-stripes) in $\text{La}_{2-x}\text{Sr}_x\text{NiO}_4$ nickelates.

It is well known that spin stripes appear in layered nickelates [7] in the doping interval $0.15 \leq x \leq 0.5$ [7]. In the doping range $0.25 < x < 0.3$ magnetic stripes and charge stripes can be easily investigated separately. In $\text{La}_{2-x}\text{Sr}_x\text{NiO}_4$ the spin-order scattering exhibits peaks in the k-space for $(1-\varepsilon; 0; l)$ with odd and even l , whereas charge-order scattering always peaks at $(2\varepsilon; 0; l)$ with odd l , [7,8] where the notation refers to the commonly used orthorhombic unit cell. We have investigated a nominal single crystal $\text{La}_{1.72}\text{Sr}_{0.28}\text{NiO}_4$ to get direct visualization of the inhomogeneity of spin stripes incommensurate order in the bulk structure from nano to micro scale.

A large number of studies on the spin stripe order in $\text{La}_{2-x}\text{Sr}_x\text{NiO}_4$ were performed by traditional neutron scattering [9–13] probing the spin ordering with low energy neutrons, which have been confirmed by muon spectroscopy [14]. Several authors have focused on both magnetic and charge order [15–20] phenomena in nickelates. Resonant elastic X-ray scattering REXS [16–18] has been used to detect spin order directly via magnetic contrast but it has no spatial resolution. Electron diffraction and hard X-ray diffraction (XRD), or non-resonant-X-ray-magnetic-scattering (NXMS) of nickelates and related magnetic materials [20–25] have been used to probe the associated tiny lattice distortions related with polaron ordering or generalized Wigner CDW and magneto-elastic strain effects [26–28]. These last methods could have spatial resolution, therefore, they open new perspectives to unveil open puzzles on the complexity of the nature of stripes in $\text{La}_{2-x}\text{Sr}_x\text{NiO}_4$ nickelates. These experiments are needed to test theories i) proposing spin stripes in strongly correlated systems including orbital and polaronic degree of freedom [26–28] and ii) the theory predicting a frustrated phase separation controlled by strain, in a strongly correlated multiband system tuned to a Lifshitz transition, in the frame of the multiband Hubbard model [29].

The accumulated data on the $\text{La}_{2-x}\text{Sr}_x\text{NiO}_4$ system [7–21] enable us to present a temperature doping phase diagram of this nickelate system in panel (a) of Figure 1. The red area indicates the antiferromagnetic order (AFM) dominating the lower Sr-doping x given by the percentage of Sr for La substitutions in the La_2O_2 plane, which is assumed to give the number of injected doped electronic holes per Ni atom in the NiO_2 plane [7]. The blue and the green areas correspond to the observation of charge-density-wave order (CDW-stripes) and magnetic spin-density-wave order (SDW-stripes), respectively. The SDW-stripes modulation wave-vector direction for $0.15 < x < 0.5$ extends in real space diagonally to the Ni-O bond direction along the b-direction of the orthorhombic unit cell. For samples with tetragonal crystal symmetry, as the one studied here, the stripe order itself breaks the rotational symmetry of the ab-plane and therefore spin stripes were assumed to show two different orientations with a 90-degree rotation around the c-axis with equal probability. The spin stripes lead to superstructure peaks either in the neutron diffraction pattern [9–13] and X-ray diffraction [16–21]. Those at the lowest momentum transfer occur at wave-vectors $(1-\varepsilon, 0, 0)$ in the orthorhombic lattice for SDW-stripes order, where ε is a temperature dependent incommensurability value, which is well separated from different charge stripe wave-vectors in the k-space.

While neutron scattering has provided for decades k-space information on spin ordering averaged over large crystal area, the present X-ray investigation reported here provides spin ordering information on illuminated spots in micron sized samples using a focused X-ray synchrotron radiation beam which allows us for the first time to detect spatial inhomogeneous spin order in a nickelate single perovskite micro-crystal. The results show large spatial fluctuations of the spin order with fractal structure indicated by power-law distribution of the spin order parameter. The particular fractal distribution is assigned to quantum criticality near an electronic topological transition or Lifshitz transition as predicted by multiband Hubbard model for strongly correlated two band systems where the strain controls the energy shift between the two bands [29].

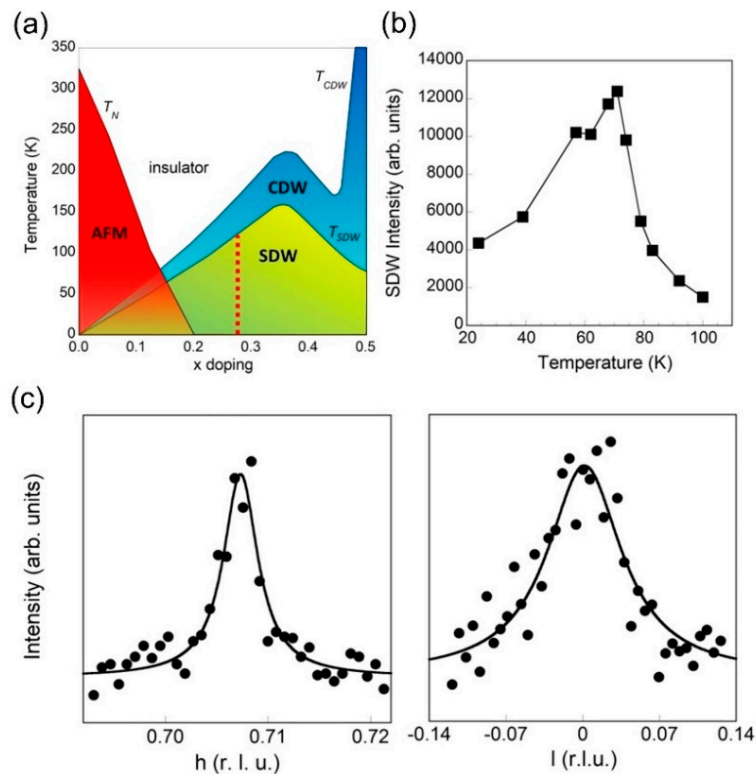


Figure 1. Phase diagram of nickelate systems and Spin-Density-Wave order. (a) Temperature-doping Phase diagram of the nickelate systems. In red the insulating Antiferromagnetic order (AFM), in blue the charge-density-wave order (CDW-strips) and in green the spin-density-wave order (SDW-strips). The red dotted line represents the temperature range where the sample of this work has been studied; (b) The intensity evolution of the SDW-stripes peak as a function of temperature; (c) SDW-stripes peak profile along the a^* (left panel) and c^* (right-panel) crystallographic directions, recorded at 30 K. The solid lines correspond to Lorentzian profiles fitted to the data, giving the in-plane and the out-of-plane correlation lengths around the average values of about 20 nm and 2 nm, respectively.

2. Materials and Methods

Single-crystalline $\text{La}_{1.72}\text{Sr}_{0.28}\text{NiO}_4$ was grown by floating zone technique. The seed and feed rods were prepared from polycrystalline powder obtained by solid state reaction of La_2O_3 , SrCO_3 and NiO with an excess of NiO . The reaction was performed at 1200 °C for 20 h with intermediate grinding. The rods were densified at 1500 °C for 5 h in air.

Micro X-ray diffraction measurements of SDW-stripes order in the sample were carried out at beamline P10 of PETRA III (DESY, Hamburg, Germany) using an energy of 8 KeV. The scattering signal was detected at a sample to detector distance of 5 m using the large horizontal scattering set-up of beamline P10 including an evacuated flight path. A PILATUS 300K detector (DECTRIS, Baden-Daettwil, Switzerland) was used to record the X-rays scattered by the sample. By employing

a focused beam with a diameter of about 1 μm and translating the sample, we mapped the spatial distribution of the $(1-\varepsilon,0,0)$ peak intensity over different areas of about $40 \times 80 \mu\text{m}^2$ in steps of 1 μm in both directions resulting in 3321 diffraction images. The scanning was performed translating the sample along the 80 horizontal lines. The exposure time for each X ray diffraction frame was of 5 s providing a X ray flux on each spot on the sample of about 10^9 count per second (cps). The time needed to collect a map was around 5 hours.

3. Results and Discussion

Scanning micro X-ray Diffraction ($S\mu\text{XRD}$) has been demonstrated to be a powerful tool in unraveling material inhomogeneity in superconductors at the micro and nanoscale, and has been successfully applied to the cuprate systems doped by oxygen interstitials: $\text{HgBa}_2\text{CuO}_{6+y}$, known as Hg1201 [4], $\text{La}_2\text{CuO}_{4+y}$, known as La124, [5,6] $\text{Bi}_2\text{Sr}_2\text{CaCu}_2\text{O}_{8+y}$, known as Bi2212 [30], $\text{YBa}_2\text{Cu}_3\text{O}_{6+y}$ known as Y123 [31–33], to iron-based superconductors [34] and to cobaltates materials opening a new era for our knowledge of quantum complex materials at nanoscale [35–79]. Here we have investigated a single crystal $\text{La}_{2-x}\text{Sr}_x\text{NiO}_4$ with Sr doping $x = 0.28$ with the spin modulation wave-vector $\varepsilon = 0.29$ consistent with the empirical relation for spin stripes wave-vector ε close to the percentage of the number of holes x per Ni sites. The red dotted line in Figure 1a represents the temperature range where the sample of this work has been studied.

In order to probe the spatial evolution of the SDW-stripes order in real space we used a micron-size X-ray beam probing the local SDW-stripes via the corresponding intensity of the magnetic so-called SDW-stripe superlattice peak at $(0.71,0)$ in the orthorhombic (h,k) plane which is well separated from the so-called CDW-stripe superlattice reflection at $(0.56,0)$.

The temperature variation of the intensity of the SDW-stripes reflection peak as a function of temperature is shown in panel (b) of Figure 1. The SDW-stripes peak is identifiable for temperatures below $T_{\text{SDW}} = 120$ K in agreement with previous works [7]. On further cooling, its integrated intensity increases, reaches a maximum around $T^* = 65$ K, followed by an intensity reduction when the temperature is further decreased as shown in Figure 1b which confirms the previous X-ray scattering results [16]. The determined temperature dependence of the SDW-stripes intensity is similar to the one reported for nickelates of different doping levels [16]. Thus, we can assume the observed behavior to be a general characteristic for SDW-stripes order. This behavior resembles what has been predicted for incommensurate cuprate stripes to occur at low temperatures, when a freezing to the lattice potential disturbs the long-range order [36–38].

The XRD diffraction peak profile of SDW-stripes shows a large anisotropy in the k -space shown in panel (c) of Figure 1. Line cuts through the SDW-stripes peak along the h -direction and l -direction, are presented in the left and right panel of Figure 1c, respectively. The solid lines correspond to results of Lorentzian profiles fitted to the data. The width of the two Lorentzian profiles gives the correlation lengths in the NiO_2 plane direction much larger than in the out-of-plane direction reflecting the quasi two-dimensionality of the magnetic interactions [7,35] in the NiO_2 atomic layer modules. In fact, this system can be described as a hetero-structure at atomic limit made of weakly interacting atomic NiO_2 layers separated by $\text{La}_{2-x}\text{Sr}_x\text{O}_2$ spacing layers. The NiO_2 layers have a sizeable compressive strain tuned by Sr doping, because of the lattice mismatch between the antiferromagnetic striped layers and the spacer layers which is a key variable controlling spin and charge ordering [51,52].

We have found an intrinsic inhomogeneous spatial organization of SDW-stripes forming stripy domains organized in micrometric stripes with different spatial arrangement as a function of temperature. In Figure 2 we report the micro X-ray diffraction maps probing the spatial inhomogeneity of the spin stripes order. Three maps were collected by scanning the same sample area at 30 K, 50 K and $T^* = 70$ K temperatures. In the spatial maps the spin-stripes peak intensity is plotted in a logarithm scale with red color areas. We observe in panels (a, b, c) of Figure 2 the formation of SDW rich regions in the sample corresponding to very high spin-stripes diffraction intensity with the shape of microscale stripes.

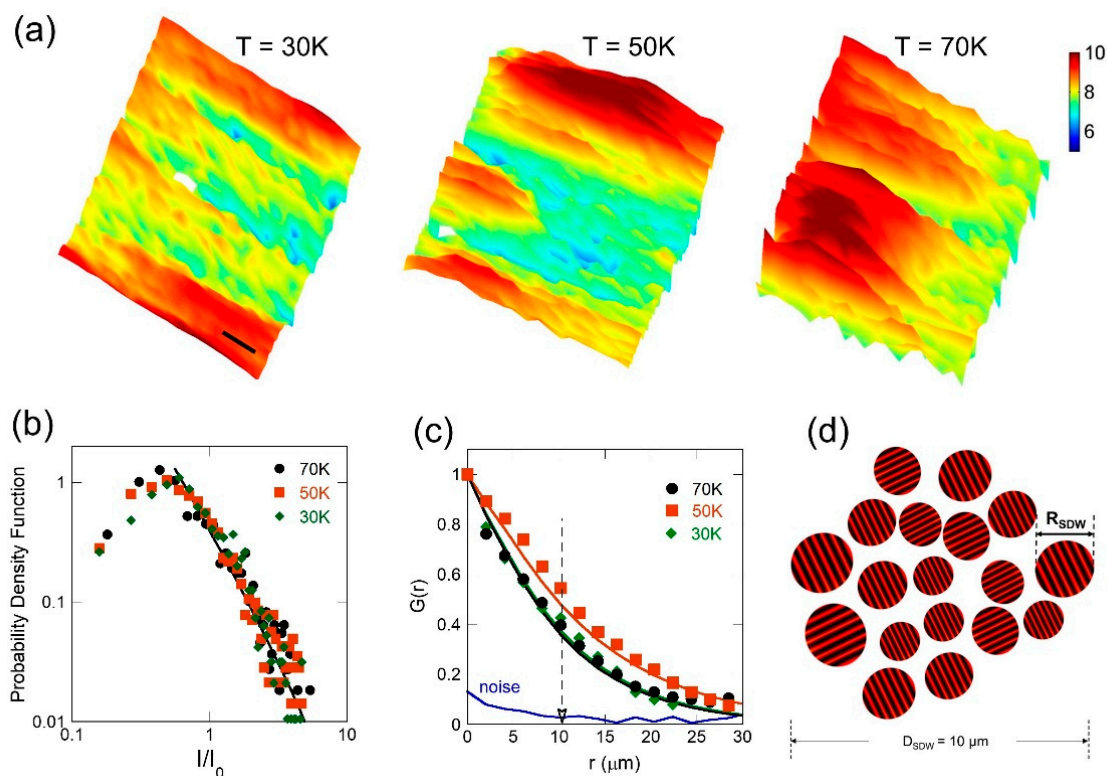


Figure 2. Spatial inhomogeneous stripes order. (a) Maps of spin stripes order showing phase segregation with spin stripes aggregates (red area) separated by regions (green-blue) with no spin stripes order signal. Each single pixel of the presented maps has been obtained recording the intensity of the XRD reflections probing SDW-strips in a specific x,y position of the sample. I . In order to reconstruct the spatial maps, the sample has been scanned over an area of about $40 \times 80 \mu\text{m}^2$ in steps of $1 \mu\text{m}$ in both directions. The black scale bar shown in the upper frame collected at 30 K corresponds to $10 \mu\text{m}$. Red areas show SDW-strips domains of the probed SDW-strips forming puddles of the order of about 10 micrometers. Blue areas are representative of SDW-strips domains where the SDW-strips signal is not detected; (b) Probability density functions of the intensity of the spin stripes signal calculated from spatial maps at 30 K, 50 K and $T^* = 70 \text{ K}$. The distributions show evident fat-tails characterized by a power-law behavior with a critical exponent of 2.1 (solid black line) which rescale on the same curve with different values of the cut-off (c). The radial correlation function $G(r)$ calculated from the three spatial maps. The blue line represents the spatial correlation obtained for a random distribution of stripes XRD peak intensities obtained by just shuffling the data. The $G(r)$ intensities decay exponentially, on the noise level, at D_{SDW} indicating the size of a typical domain of 10 microns made by aggregation of individual nanoscale stripes puddles in the NiO_2 in the ab -plane; (d) Pictorial view of the stripes puddles of about $R_{SDW} \approx 20 \text{ nm}$, given by the correlation length extracted from the width of the diffraction reflection lines (see Figure 1), forming aggregates of about $D_{SDW} \approx 10 \mu\text{m}$ size below the critical temperature T^* .

The microscale spin rich stripes are separated by blue or green areas where the spin diffraction signal is the noise level. The two regions are separated by the yellow interface domains between red micro-scale stripes with spin modulations, and blue-green regions with no spin stripe modulation. The red spin stripes as a function of temperature shows a maximum density at $T^* = 70 \text{ K}$ and by decreasing the temperature some of the red color spin stripes disappear and are replaced by the increasing blue-green regions with missing SDW.

Panel (b) in Figure 2b shows the statistical analysis of the distribution of the SDW-strips intensity, I , in terms of the probability density function $P(x)$ where $x = I/I_0$ and I_0 is the average intensity of the

map. The intensity distributions strongly deviate from a Gaussian distribution and show extended fat tails which can be fitted by an exponentially truncated power-law behavior

$$P(x) = x^{-\alpha} \exp(-x/x_\tau)$$

with a critical exponent $\alpha = 2.1 \pm 0.2$ and cut-off $x_\tau = 7 \pm 0.5$ at $T^* = 70$ K shown by a solid line in panel (b). Similar behavior has been reported for the distribution of the oxygen interstitials and the CDW order accompanied by local lattice distortions in the active layers of cuprates and related materials [4–6,30–34]. This result underlines a spatial organization of the spin stripes order in “scale-free” or fractal-like geometries showing long-range power-law correlations common to systems showing fractal geometry which are quantified by the experimentally determined critical exponent α and the cut-off x_τ . This physical state appears in systems “tuned” near a quantum critical point which is a feature of striped quantum complex matter phase in perovskite materials [4–6,30–34].

For investigating the spatial distribution of the microscale SDW-strip we have calculated the radial distribution function $G(r)$ of the XRD reflection intensity in the spatial maps at the three temperatures reported in panel (c) in Figure 2. All the $G(r)$ curves show a similar exponential decay falling on the noise level at distances with $D_{SDW} = 10 \mu\text{m}$. We associate this length to the average size of the microscale SDW-strip domain. The average size R_{SDW} of the nano-spin-puddles in the ab-plane deduced by the diffraction profile width in Figure 1 is of the order of 20 nm, therefore, each illuminated $1 \mu\text{m}$ spot in our scanning mode provides the average value over about 2.5×10^3 nano-spin-puddles. A pictorial view of spin-rich domain of radius $D_{SDW} = 10 \mu\text{m}$ hosting about 2.5×10^5 nano-spin-puddles of radius R_{SDW} is shown in panel (d) of Figure 2.

4. Conclusions

In this paper we have provided experimental evidence for spatial phase separation of magnetic stripes order in nickelates predicted for two bands strongly correlated systems near a Lifshitz transition [29]. In cuprates and related matter the coexistence of spin ordered, charge ordered and lattice ordered puddles [39–41] have pointed towards the possibility of quantum complex fluids at the interfaces spanning filamentary hyperbolic spaces [42] as it has been found in functional biological matter [43,44]. Moreover, it is possible that the doped charges in nickelates form polaron [45] anisotropic aggregates [46] with associated tilts [47] making quantum networks [48] of polarons. Therefore, the phase separation reported in this work could be assigned also to the liquid-stripped liquid phase separation in liquids of anisotropic polarons similar to the liquid-stripped liquid phase separation in water [49,50]. The anisotropy of polaron clusters in nickelates is assigned here to misfit strain [51,52] and orbital degrees of freedom [53–55]. The detection of the complex magnetic structures in strongly correlated electron systems by X-ray diffraction [56,57] can be used to support the association of the spin signal to polaronic distortions. The new mesoscopic phase separation with scale free spatial correlation for spin stripes order found here in nickelates is in agreement with previous indications [53–59] and it provides the experimental smoking gun evidence that the spin ordering in spin stripes phase in nickelates is near a quantum critical point. A similar spatial fractal landscape has been found in cuprates [46–52] and in other oxides near a quantum phase transition as in VO_2 [60–63], in ruthenates [64,65], and in diborides [66,67]. The observed scale free phase separation in nickelates is in agreement with the predictions by of the multiband Hubbard model of frustrated phase separation in strongly correlated two bands systems [29,68]. In this regime the strain manipulation provides a key physical variable [51,52] to drive the system near a particular quantum critical point at Lifshitz transitions or topological electronic transitions. Further experimental work is needed to clarify if hyperbolic space correlations predicted by theory [69,70] and observed in correlated metallic cuprates [4,42] are present or not in the stripes spatial landscape in nickelates. Finally, we have reported new information on the quantum complex scenario near criticality in nickelates which opens new venues to applications and developments of new magnetic and electronic devices. In fact, in the

proximity of a topological Lifshitz transition it is possible to control novel macroscopic functionalities by a weak external stimulus such as stress [25–36,71–75], current density [64,65] or photon illumination dose [5,76–79].

Author Contributions: A.R. conceived the project and designed all the experiments. C.S.-L., M.S. and G.C. contributed to the planning of the experiments. The samples were grown by A.A.N., and characterized by M.B. (Marcel Buchholz), C.T., C.S.-L. and M.B. (Markus Braden); preliminary measurements using soft X-ray have been performed at ALS (Berkeley) by A.R., S.M., J.L., L.M. and S.R. and at P04-PETRA III (DESY) by M. B. (Marcel Buchholz), C.S.-L. and J.V.; micro X-ray diffraction experiments have been carried out at P10-PETRA III (DESY) by A.R., G.C., N.P., B.J., A.Z. and M.S.; data analysis has been done by A.R., G.C., A.B., N.P., M.B. ((Markus Braden)), C.S.-L., A.R. and M.S. discussed the results and worked on the interpretation of the data. The manuscript has been written by A.R., G.C. and A.B. collecting feedback from all the authors.

Funding: This research was supported by the Helmholtz Virtual Institute: Dynamic Pathways in Multidimensional Landscapes. A.R. and G.C. acknowledge the Stephenson Distinguished Visitor Program by DESY. N.P. acknowledges the Italian Ministry for Education and Research and Marie Curie IEF project for partial financial support. A.A.N. acknowledges funding from Ministry of Research, Technology and Higher Education through Hibah WCU-ITB. Work in Cologne was supported by the DFG through SFB608 and by the German Ministry for Science and Education through contract 05K10PK2. Moreover, support by the DFG within SFB 925 and by the Superstripes-onlus is gratefully acknowledged. Work at the ALS, LBNL was supported by the Director, Office of Science, Office of Basic Energy Sciences, of the US Department of Energy (Contract No. DE-AC02-05CH11231).

Conflicts of Interest: The authors declare no conflict of interest.

References

1. Dagotto, E. Complexity in strongly correlated electronic systems. *Science* **2005**, *309*, 257–262. [[CrossRef](#)] [[PubMed](#)]
2. Vojta, M. Lattice symmetry breaking in cuprate superconductors: Stripes, nematics and superconductivity. *Adv. Phys.* **2009**, *58*, 699–820. [[CrossRef](#)]
3. Bianconi, A.; Saini, N.L. *Stripes and Related Phenomena*; Springer Science Business Media: Berlin, Germany, 2001.
4. Campi, G.; Bianconi, A.; Poccia, N.; Barbo, G.; Arrighetti, G.; Innocenti, D.; Karpinski, J.; Zhigadlo, D.N.; Kazakov, S.M.; Burghammer, M.; et al. Inhomogeneity of charge-density-wave order and quenched disorder in a high- T_c superconductor. *Nature* **2015**, *525*, 359–362. [[CrossRef](#)] [[PubMed](#)]
5. Poccia, N.; Ricci, A.; Campi, G.; Fratini, M. Optimum inhomogeneity of local lattice distortions in $\text{La}_2\text{CuO}_{4+y}$. *Proc. Natl. Acad. Sci. U.S.A.* **2012**, *109*, 15685–15690. [[CrossRef](#)] [[PubMed](#)]
6. Fratini, M.; Poccia, N.; Ricci, A.; Campi, G.; Burghammer, M.; Aeppli, G.; Bianconi, A. Scale-free structural organization of oxygen interstitials in $\text{La}_2\text{CuO}_{4+y}$. *Nature* **2010**, *466*, 841–844. [[CrossRef](#)] [[PubMed](#)]
7. Ulbrich, H.; Braden, M. Neutron scattering studies on stripe phases in non-cuprate materials. *Phys. C Supercond.* **2012**, *481*, 31–45. [[CrossRef](#)]
8. Lee, S.H.; Cheong, S.W. Melting of quasi-two-dimensional charge stripes in $\text{La}_{5/3}\text{Sr}_{1/3}\text{NiO}_4$. *Phys. Rev. Lett.* **1997**, *79*, 2514. [[CrossRef](#)]
9. Yoshizawa, H.; Kakeshita, T.; Kajimoto, R.; Tanabe, T.; Katsufuji, T.; Tokura, Y. Stripe order at low temperatures in $\text{La}_{2-x}\text{Sr}_x\text{NiO}_4$ with $0.289 \leq x \leq 0.5$. *Phys. Rev. B* **2000**, *61*, R854. [[CrossRef](#)]
10. Kajimoto, R.; Kakeshita, T.; Yoshizawa, H.; Tanabe, T.; Katsufuji, T.; Tokura, Y. Hole concentration dependence of the ordering process of the stripe order in $\text{La}_{2-x}\text{Sr}_x\text{NiO}_4$. *Phys. Rev. B* **2001**, *64*, 144432. [[CrossRef](#)]
11. Lee, S.H.; Cheong, S.W.; Yamada, K.; Majkrzak, C.F. Charge canted spin order in $\text{La}_{2-x}\text{Sr}_x\text{NiO}_4$ ($x = 0.275, 1/3$). *Phys. Rev. B* **2001**, *63*, 060405. [[CrossRef](#)]
12. Boothroyd, A.T.; Freeman, P.G.; Prabhakaran, D.; Enderle, M.; Kulda, J. Magnetic order and dynamics in stripe-ordered $\text{La}_{2-x}\text{Sr}_x\text{NiO}_4$. *Phys. B Condens. Matter* **2004**, *345*, 1–5. [[CrossRef](#)]
13. Freeman, P.G.; Christensen, N.B.; Prabhakaran, D.; Boothroyd, A.T. The temperature evolution of the out-of-plane correlation lengths of charge-stripe ordered $\text{La}_{1.725}\text{Sr}_{0.275}\text{NiO}_4$. *J. Phys. Conf. Ser.* **2010**, *200*, 012037. [[CrossRef](#)]
14. Chow, K.H.; Pattenden, P.; Blundell, S.J.; Hayes, W. Muon-spin-relaxation studies of magnetic order in heavily doped $\text{La}_{2-x}\text{Sr}_x\text{NiO}_{4+\delta}$. *Phys. Rev. B* **1996**, *53*, R14725. [[CrossRef](#)] [[PubMed](#)]
15. Schüßler-Langeheine, C.; Schlappa, J.; Tanaka, A.; Hu, Z.; Chang, C.F.; Schierle, E.; Benomar, M.; Ott, H.; Weschke, E.; Kaindl, G.; et al. Spectroscopy of stripe order in $\text{La}_{1.8}\text{Sr}_{0.2}\text{NiO}_4$ using resonant soft X-ray diffraction. *Phys. Rev. Lett.* **2005**, *95*, 156402. [[CrossRef](#)] [[PubMed](#)]

16. Schlappa, J.; Chang, C.F.; Schierie, E.; Tanaka, A. Static and fluctuating stripe order observed by resonant soft X-ray diffraction in $\text{La}_{1.8}\text{Sr}_{0.2}\text{NiO}_4$. *arXiv* **2009**, arXiv:0903.0994v1.
17. Coslovich, G.; Huber, B.; Lee, W.S.; Chuang, Y.D.; Zhu, Y.; Sasagawa, T.; Hussain, Z.; Bechtel, H.A.; Martin, M.C.; Shen, Z.X.; et al. Ultrafast charge localization in a stripe-phase nickelate. *Nature Commun.* **2013**, *4*, 2643. [[CrossRef](#)]
18. Wilkins, S.B.; Hatton, P.D.; Liss, K.D.; Ohler, M.; Katsufuji, T.; Cheong, S.W. High-resolution high energy X-ray diffraction studies of charge ordering in CMR manganites and nickelates. *Int. J. Mod. Phys. B* **2000**, *14*, 3753–3758. [[CrossRef](#)]
19. Chen, C.H.; Cheong, S.W.; Cooper, A.S. Charge modulations in $\text{La}_{2-x}\text{Sr}_x\text{NiO}_{4+y}$ ordering of polarons. *Phys. Rev. Lett.* **1993**, *71*, 2461. [[CrossRef](#)]
20. Ghazi, M.E.; Spencer, P.D.; Wilkins, S.B.; Hatton, P.D.; Mannix, D.; Prabhakaran, D. Incommensurate charge stripe ordering in $\text{La}_{2-x}\text{Sr}_x\text{NiO}_4$ for $x = (0.33, 0.30, 0.275)$. *Phys. Rev. B* **2004**, *70*, 144507. [[CrossRef](#)]
21. Du, C.H.; Ghazi, M.E.; Su, Y.X.; Pape, I. Critical Fluctuations and quenched Disordered Two-Dimensional Charge Stripes in $\text{La}_{5/3}\text{Sr}_{1/3}\text{NiO}_4$. *Phys. Rev. Lett.* **2000**, *84*, 3911. [[CrossRef](#)]
22. Johnson, R.D.; Mazzoli, C.; Bland, S.R.; Du, C. Magnetically induced electric polarization reversal in multiferroic TbMn_2O_5 : Terbium spin reorientation studied by resonant X-ray diffraction. *Phys. Rev. B* **2011**, *83*, 054438. [[CrossRef](#)]
23. Vecchini, C.; Bombardi, A.; Chapon, L.C.; Lee, N.; Radaelli, P.G.; Cheong, S.W. Magnetic phase diagram and ordered ground state of GdMn_2O_5 multiferroic studied by X-ray magnetic scattering. *J. Phys. Conf. Ser.* **2014**, *519*, 012004. [[CrossRef](#)]
24. Pincini, D.; Boseggia, S.; Perry, R.; Gutmann, M. Persistence of antiferromagnetic order upon La substitution in the Mott insulator Ca_2RuO_4 . *Phys. Rev. B* **2018**, *98*, 014429. [[CrossRef](#)]
25. Price, N.W.; Vibhakar, A.M.; Johnson, R.D.; Schad, J.; Saenrang, W.; Bombardi, A.; Chmiel, F.P.; Eom, C.B.; Radaelli, P.G. Strain engineering a multiferroic monodomain in thin-film BiFeO_3 . *Phys. Rev. Appl.* **2019**, *11*, 024035. [[CrossRef](#)]
26. Caprara, S.; Sulpizi, M.; Bianconi, A.; Castro, C. Single-particle properties of a model for coexisting charge and spin quasicritical fluctuations coupled to electrons. *Phys. Rev. B* **1999**, *59*, 14980. [[CrossRef](#)]
27. Carlson, E.W.; Yao, D.X.; Campbell, D.K. Spin waves in striped phases. *Phys. Rev. B* **2004**, *70*, 064505. [[CrossRef](#)]
28. Raczkowski, M.; Fresard, R.; Oles, A.M. Microscopic origin of diagonal stripe phases in doped nickelates. *Phys. Rev. B* **2006**, *73*, 094429. [[CrossRef](#)]
29. Bianconi, A.; Poccia, N.; Sboyshakov, A.O.; Rakhmanov, A.L.; Kugel, K.I. Intrinsic arrested nanoscale phase separation near a topological Lifshitz transition in strongly correlated two-band metals. *Supercond. Sci. Technol.* **2015**, *28*, 024005. [[CrossRef](#)]
30. Poccia, N.; Campi, G.; Fratini, M.; Ricci, A. Spatial inhomogeneity and planar symmetry breaking of the lattice incommensurate supermodulation in the high-temperature superconductor $\text{Bi}_2\text{Sr}_2\text{CaCu}_2\text{O}_{8+y}$. *Phys. Rev. B* **2011**, *84*, 100504. [[CrossRef](#)]
31. Ricci, A.; Poccia, N.; Campi, G.; Coneri, F.; Caporale, A.S.; Innocenti, D.; Burghammer, M.; Zimmermann, M.V.; Bianconi, A. Multiscale distribution of oxygen puddles in 1/8 doped $\text{YBa}_2\text{Cu}_3\text{O}_{6.67}$. *Sci. Rep.* **2013**, *3*, 2383. [[CrossRef](#)]
32. Ricci, A.; Poccia, N.; Campi, G.; Coneri, F.; Barba, L.; Arrighetti, G.; Polentarutti, M.; Burghammer, M.; Sprung, M.; Zimmermann, M.V.; et al. Networks of superconducting nano-puddles in 1/8 doped $\text{YBa}_2\text{Cu}_3\text{O}_{6.5+y}$ controlled by thermal manipulation. *New J. Phys.* **2014**, *16*, 053030. [[CrossRef](#)]
33. Campi, G.; Ricci, A.; Poccia, N.; Barba, L.; Arrighetti, G.; Burghammer, M.; Caporale, A.S.; Bianconi, A. Scanning micro-X-ray diffraction unveils the distribution of oxygen chain nanoscale puddles in $\text{YBa}_2\text{Cu}_3\text{O}_{6.33}$. *Phys. Rev. B* **2013**, *87*, 014517. [[CrossRef](#)]
34. Ricci, A.; Poccia, N.; Joseph, B.; Innocenti, D. Direct observation of nanoscale interface phase in the superconducting chalcogenide $\text{K}_x\text{Fe}_{2-y}\text{Se}_2$ with intrinsic phase separation. *Phys. Rev. B* **2015**, *91*, 020503. [[CrossRef](#)]
35. Drees, Y.; Li, Z.W.; Ricci, A.; Rotter, M.; Schmidt, W.; Lamago, D.; Sobolev, O.; Rutt, U.; Gutowski, O.; Sprung, M.; et al. Hour-glass magnetic excitations induced by nanoscopic phase separation in cobalt oxides. *Nature Commun.* **2014**, *5*, 573. [[CrossRef](#)]

36. Mu, Y.; Ma, Y. Self-organizing stripe patterns in two-dimensional frustrated systems with competing interactions. *Phys. Rev. B* **2003**, *67*, 014110. [[CrossRef](#)]
37. Schmalian, J.; Wolynes, P.G. Stripe glasses: Self-generated randomness in a uniformly frustrated system. *Phys. Rev. Lett.* **2000**, *85*, 836. [[CrossRef](#)]
38. Bogner, S.; Scheidl, S. Pinning of stripes in cuprate superconductors. *Phys. Rev. B* **2001**, *64*, 054517. [[CrossRef](#)]
39. Poccia, N.; Chorro, M.; Ricci, A.; Xu, W.; Marcelli, A.; Campi, G.; Bianconi, A. Percolative superconductivity in $\text{La}_2\text{CuO}_{4.06}$ by lattice granularity patterns with scanning micro X-ray absorption near edge structure. *Appl. Phys. Lett.* **2014**, *104*, 221903. [[CrossRef](#)]
40. Bianconi, A.; Di Castro, D.; Bianconi, G.; Pifferi, A.; Saini, N.L.; Chou, F.C.; Johnston, D.C.; Colapietro, M. Coexistence of stripes and superconductivity: T_c amplification in a superlattice of superconducting stripes. *Phys. C: Supercond.* **2000**, *341*, 1719–1722. [[CrossRef](#)]
41. Chen, X.; Schmehr, J.L.; Islam, Z.; Porter, Z.; Zoghlin, E.; Finkelstein, K.; Ruff, J.P.C.; Wilson, S.D. Unidirectional spin density wave state in metallic $(\text{Sr}_{1-x}\text{La}_x)_2\text{IrO}_4$. *Nat. Commun.* **2018**, *9*, 103. [[CrossRef](#)]
42. Campi, G.; Bianconi, A. High-Temperature superconductivity in a hyperbolic geometry of complex matter from nanoscale to mesoscopic scale. *J. Supercond. Nov. Magn.* **2016**, *29*, 627–631. [[CrossRef](#)]
43. Campi, G.; Di Gioacchino, M.; Poccia, N.; Ricci, A.; Burghammer, A.; Ciasca, G.; Bianconi, A. Nanoscale correlated disorder in out-of-equilibrium myelin ultrastructure. *ACS Nano* **2017**, *12*, 729–739. [[CrossRef](#)]
44. Campi, G.; Cristofaro, F.; Pani, G.; Fratini, M.; Pascucci, B.; Corsetto, P.A.; Weinhausen, B.; Cedola, A.; Rizzo, A.M.; Visai, L.; et al. Heterogeneous and self-organizing mineralization of bone matrix promoted by hydroxyapatite nanoparticles. *Nanoscale* **2017**, *9*, 17274–17283. [[CrossRef](#)]
45. Zaanen, J.; Littlewood, P.B. Freezing electronic correlations by polaronic instabilities in doped La_2NiO_4 . *Phys. Rev. B* **1994**, *50*, 7222. [[CrossRef](#)]
46. Kusmartsev, F.V.; Di Castro, D.; Bianconi, G.; Bianconi, A. Transformation of strings into an inhomogeneous phase of stripes and itinerant carriers. *Phys. Lett. A* **2000**, *275*, 118–123. [[CrossRef](#)]
47. Gavrichkov, V.A.; Shanko, Y.; Zamkova, N.G.; Bianconi, A. Is There Any Hidden Symmetry in Stripe Structure of Perovskite High-Temperature Superconductors? *J. Phys. Chem. Lett.* **2019**, *10*, 1840–1844. [[CrossRef](#)]
48. Bianconi, G. Quantum statistics in complex networks. *Phys. Rev. E* **2002**, *66*, 056123. [[CrossRef](#)]
49. Innocenti, D.; Ricci, A.; Poccia, N.; Campi, G.; Fratini, M.; Bianconi, A. A model for liquid-striped liquid phase separation in liquids of anisotropic polarons. *J. Supercond. Nov. Magn.* **2009**, *22*, 529–533. [[CrossRef](#)]
50. Campi, G.; Innocenti, D.; Bianconi, A. CDW and similarity of the Mott insulator-to-metal transition in cuprates with the gas-to-liquid-liquid transition in supercooled water. *J. Supercond. Nov. Magn.* **2015**, *28*, 1355–1363. [[CrossRef](#)]
51. Agrestini, S.; Saini, N.L.; Bianconi, G.; Bianconi, A. The strain of CuO_2 lattice: The second variable for the phase diagram of cuprate perovskites. *J. Phys. A Math. Gen.* **2003**, *36*, 9133. [[CrossRef](#)]
52. Bianconi, A.; Agrestini, S.; Bianconi, G.; Di Castro, D.; Saini, N.L. A quantum phase transition driven by the electron lattice interaction gives high T_c superconductivity. *J. Alloy. Compd.* **2001**, *317*, 537–541. [[CrossRef](#)]
53. Lichtenstein, A.I.; Fleck, M.; Oles, A.M.; Hedin, L. Dynamical mean-field theory of stripe ordering. In *Stripes and Related Phenomena*; Bianconi, A., Saini, N.L., Eds.; Springer: Boston, MA, USA, 2002; pp. 101–109.
54. Raczkowski, M.; Oleś, A.M. Competition between vertical and diagonal stripes in the Hartree-Fock approximation. *AIP Conf. Proc.* **2003**, *678*, 293–302.
55. Oles, A.M. Charge and orbital order in transition metal oxides. *Acta Phys. Polon. A* **2010**, *118*, 212. [[CrossRef](#)]
56. Beale, T.A.W.; Wilkins, S.B.; Johnson, R.D.; Prabhakaran, D.; Boothroyd, A.T.; Steadman, P.; Dhesi, S.S.; Hatton, P.D. Advances in the understanding of multiferroics through soft X-ray diffraction. *Eur. Phys. J. Spec. Top.* **2012**, *208*, 99–106. [[CrossRef](#)]
57. Radaelli, P.G.; Dhesi, S.S. The contribution of Diamond light source to the study of strongly correlated electron systems and complex magnetic structures. *Philos. Trans. R. Soc. A Math. Phys. Eng. Sci.* **2015**, *373*, 20130148. [[CrossRef](#)]
58. Mattoni, G.; Zubko, P.; Maccherozzi, F.; van der Torren, A.J.H.; Boltje, D.B.; Hadjimichael, M.; Manca, N.; Catalano, S.; Gibert, M.; Liu, Y.; et al. Striped nanoscale phase separation at the metal-insulator transition of heteroepitaxial nickelates. *Nat. Commun.* **2016**, *7*, 13141. [[CrossRef](#)]
59. Varignon, J.; Grisolia, M.N.; Íñiguez, J.; Barthelémy, A.; Bibes, M. Complete phase diagram of rare-earth nickelates from first-principles. *NPJ Quantum Mater.* **2017**, *2*, 21. [[CrossRef](#)]

60. Liu, M.; Sternbach, A.J.; Wagner, M.; Slusar, T.V.; Kong, T.; Budko, S.L.; Salinporn, K.; Qazibash, M.M.; McLeod, A.; Fei, Z.; et al. Phase transition in bulk single crystals and thin films of VO₂ by nanoscale infrared spectroscopy and imaging. *Phys. Rev. B* **2015**, *91*, 245155. [[CrossRef](#)]
61. Bianconi, A. Multiplet splitting of final-state configurations in X-ray-absorption spectrum of metal VO₂: Effect of core-hole-screening, electron correlation and metal-insulator transition. *Phys. Rev. B* **1982**, *26*, 2741. [[CrossRef](#)]
62. Marcelli, A.; Coreno, M.; Stredansky, M.; Xu, W. Nanoscale phase separation and lattice complexity in VO₂: The metal–insulator transition investigated by XANES via Auger electron yield at the vanadium L₂₃-edge and resonant photoemission. *Condens. Matt.* **2017**, *2*, 38. [[CrossRef](#)]
63. Gioacchino, D.; Marcelli, A.; Puri, A.; Zou, C. Metastability phenomena in VO₂ thin films. *Condens. Matt.* **2017**, *2*, 10. [[CrossRef](#)]
64. Zhang, J.; McLeod, A.S.; Han, Q.; Chen, X.; Bechtel, H.A.; Yao, Z.; Gilbert, S.N.; Ciavatti, T.; Tao, T.H.; Aronson, M.; et al. Nano-resolved current-induced insulator-metal transition in the Mott insulator Ca₂RuO₄. *Phys. Rev. X* **2019**, *9*, 011032. [[CrossRef](#)]
65. Luo, Y.; Pustogow, A.; Guzman, P.; Dioguardi, A.P.; Thomas, S.M.; Ronning, F.; Kikugawa, N.; Sokolov, D.A.; Jerzebeck, A.P.; Mackenzie, A.P.; et al. Normal state O¹⁷ NMR studies of Sr₂RuO₄ under uniaxial stress. *Phys. Rev. X* **2019**, *9*, 021044.
66. Bauer, E.; Paul, C.; Berger, S.; Majumdar, S.; Michor, H.; Giovannini, M.; Saccone, A.; Binaconi, A. Thermal conductivity of superconducting MgB₂. *J. Phys. Condens. Matt.* **2001**, *13*, L487. [[CrossRef](#)]
67. Agrestini, S.; Metallo, C.; Filippi, M.; Simonelli, L.; Gampi, G.; Sanipoli, C.; Liarokapis, E.; De Negri, S.; Giovannini, M.; Saccone, A.; et al. Substitution of Sc for Mg in MgB₂: Effects on transition temperature and Kohn anomaly. *Phys. Rev. B* **2004**, *70*, 134514. [[CrossRef](#)]
68. Kugel, K.I.; Rakhmanov, A.L.; Sboyshakov, A.O.; Kusmartsev, F.V.; Poccia, N.; Bianconi, A. A two-band model for the phase separation induced by the chemical mismatch pressure in different cuprate superconductors. *Supercond. Sci. Technol.* **2008**, *22*, 014007. [[CrossRef](#)]
69. Bianconi, G.; Rahmede, C. Emergent hyperbolic network geometry. *Sci. Rep.* **2017**, *7*, 41974. [[CrossRef](#)]
70. Bianconi, G.; Ziff, R.M. Topological percolation on hyperbolic simplicial complexes. *Phys. Rev. E* **2018**, *98*, 052308. [[CrossRef](#)]
71. Kagan, M.Y.; Bianconi, A. Fermi-Bose mixtures and BCS-BEC crossover in high-T_c superconductors. *Condens. Matt.* **2019**, *4*, 51. [[CrossRef](#)]
72. Yanagisawa, T. Mechanism of high-temperature superconductivity in correlated-electron systems. *Condens. Matt.* **2019**, *4*, 57. [[CrossRef](#)]
73. Jurkutat, M.; Erb, A.; Haase, J. T_c and other cuprate properties in relation to planar charges as measured by NMR. *Condens. Matt.* **2019**, *4*, 67. [[CrossRef](#)]
74. Caprara, S. The ancient romans' route to charge density waves in cuprates. *Condens. Matt.* **2019**, *4*, 60. [[CrossRef](#)]
75. Yamamoto, S.; Fujiwara, T.; Hatsugai, Y. Electronic structure of charge and spin stripe order in La_{2-x}Sr_xNiO₄ (x=1/3,1/2). *Phys. Rev. B* **2007**, *76*, 165114. [[CrossRef](#)]
76. Campi, G.; Castro, D.D.; Bianconi, G.; Agrestini, A.; Saini, N.L.; Oyanagi, H.; Bianconi, A. Photo-Induced phase transition to a striped polaron crystal in cuprates. *Phase Transit.* **2002**, *75*, 927–933. [[CrossRef](#)]
77. Campi, G.; Dell'Omo, C.; Di Castro, D.; Agrestini, S.; Filippi, M.; Bianconi, G.; Barba, L.; Cassetta, A.; Colapietro, M.; Saini, N.L.; et al. Effect of temperature and X-ray illumination on the oxygen ordering in La₂CuO_{4.1} Superconductor. *J. Supercond.* **2004**, *17*, 137–142. [[CrossRef](#)]
78. Poccia, N.; Bianconi, A.; Campi, G.; Fratini, M.; Ricci, A. Size evolution of the oxygen interstitial nanowires in La₂CuO_{4+y} by thermal treatments and X-ray continuous illumination. *Superconductor Sci. Technol.* **2012**, *25*, 124004. [[CrossRef](#)]
79. Campi, G.; Ricci, A.; Poccia, N.; Fratini, M.; Bianconi, A. X-rays Writing/Reading of charge density waves in the CuO₂ plane of a simple cuprate superconductor. *Condens. Matt.* **2017**, *2*, 26. [[CrossRef](#)]

